Supplementary Materials: Electrochemo-Mechanical Coupled Behaviors in Sodium-Ion Batteries Upon Stack Pressure

Bo Rui[1, 2], Youngwon Hahn[3], Amit Bhowmick[1,2], Farzaneh Mousavi[3], Sandeep Kulathu[3], Victor Oancea[3], and Jun Xu[1,2, 4*]

[1]*Department of Mechanical Engineering, University of Delaware, Newark, DE 19716, USA*

[2]*Energy Mechanics and Sustainability Laboratory (EMSLab), University of Delaware, Newark, DE 19716, USA*

[3]*Dassault Systèmes Americas Corp., 1301 Atwood Ave, Suite 101W, Johnston, RI 02919, USA*

[4]*Data Science Institute, University of Delaware, Newark, DE 19716, USA*

[*] Corresponding to: Prof. Jun Xu at junxu@udel.edu

Table. S1 Geometry of the jellyroll

Parameters	Values	Source
3D geometry of the jellyroll		
t^j	5.6 mm	Measured
w^j	18.2 mm	Measured
δ^c	0.122 mm	Measured
δ^a	0.247 mm	Measured
δ^{se}	0.018 mm	Measured
δ^{pc}	0.015 mm	Measured
δ^{nc}	0.012 mm	Measured

Table. S2 The main equations of the governing computational framework [1–7]

Mechanical model	
Function name	Function
Mechanical equilibrium	$\nabla \cdot \boldsymbol{\sigma} + \mathbf{b} = 0$
Constitutive relation	$\sigma = \mathbf{D}^{el} : (\boldsymbol{\varepsilon} - \boldsymbol{\varepsilon}^{eig}) = \mathbf{D}^{el} : \boldsymbol{\varepsilon}^{el}$
Electrochemical model	
Solid potential	$i_s = -\sigma_s^{\text{eff}} \nabla \phi_s$
Electrolyte potential	$i_e = -\sigma_e^{\text{eff}} \nabla \phi_e + \frac{2\sigma_e^{\text{eff}} RT}{F}\left(1 + \frac{d \ln f}{d \ln c_i}\right)(1 - t_+)\nabla \ln c_e$
Transport in solid	$\frac{\partial c_s}{\partial t} = D_s \frac{1}{r^2}\frac{\partial}{\partial r}\left(r^2 \frac{\partial c_s}{\partial r}\right)$
Boundary conditions	$\frac{\partial c_s}{\partial r}\Big\|_{r=0} = 0,\ -D_s \frac{\partial c_s}{\partial r}\Big\|_{r=r_s} = \frac{j^{Li}}{a_s F}$
Transport in the electrolyte	$\varepsilon_e \frac{\partial c_e}{\partial t} = \nabla \cdot \left(D_e^{\text{eff}} \nabla c_e\right) + \frac{a j_{\text{loc}}}{F}(1 - t_+)$
Reaction rate	$j_{\text{loc}} = j_0 \left\{ \exp\left(\frac{\alpha^{\text{ng}} \eta F}{R_g T}\right) - \exp\left(\frac{-\alpha^{\text{ps}} \eta F}{R_g T}\right) \right\}$
Overpotential	$\eta = \phi_s - \phi_e - U$
Initial condition	$c_e = c_e^0,\ c_s = c_s^0,\ T = T^0$

Table. S3 The material parameters of the SIBs

Parameters	Unit	Cathode	Separator	Anode
Density	kg/m^3	$\rho^{Al} = 2770$ $\rho^{c} = 2900$ [a]	$\rho^{se} = 817.7$ [c]	$\rho^{Al} = 2770$ $\rho^{a} = 800$ [a]
Elastic constants	MPa	$E^{c} = 2275$ [c]	$E^{se} = 555$ [c]	$E^{a} = 2260$ [c]
Poisson' ratio	1	$v^{c} = 0.3$	$v^{se} = 0.3$	$v^{a} = 0.3$
Electrical conductivity	S/m	$\kappa^{c} = 50$ [8]	$\kappa^{se} = 0.7325$	$\kappa^{a} = 256$ [8]
Diffusion coefficient	m^2/s	$D^{c}\left(c_{\mathrm{NNMF}}\right)$[b]	$D^{se} = 1.81\times10^{-10}$	$D^{a}\left(c_{\mathrm{HC}}\right)$[b]
Maximum concentration	mol/m^3	$c_{eq}^{c} = 15148$ [a]		$c_{eq}^{a} = 8357$ [a]
Equilibrium potential	V	$E_{eq}^{c}\left(c_{\mathrm{NNMF}}\right)$[9]		$E_{eq}^{a}\left(c_{\mathrm{HC}}\right)$[8]
Rate constant	m/s	$k^{c}\left(c_{\mathrm{NNMF}}\right)$[b]		$k^{a}\left(c_{\mathrm{HC}}\right)$[b]

[a] Directly from manufacturer's data or calculated

[b] Calibrated by experimental results

[c] Measured

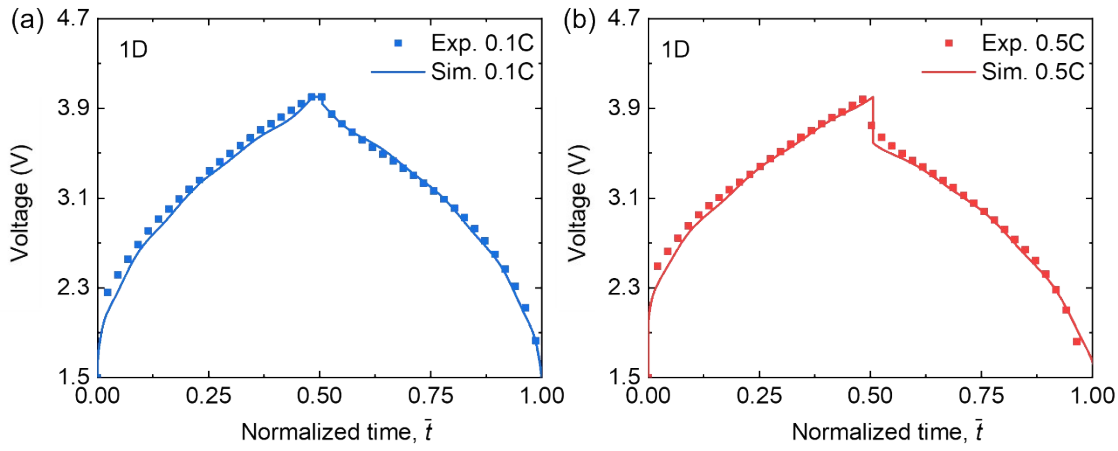

Fig. S1 Model validation of sodium-ion batteries. (a) Comparison between experimental measurements and one-dimensional (1D) model predictions of voltage evolution during charge–discharge at 0.1C. (b) Experimental and simulated voltage profiles at a higher rate of 0.5C, demonstrating the model's capability to capture rate-dependent electrochemical behavior. Here, normalization is performed using the full-cycle duration at the corresponding C-rate.

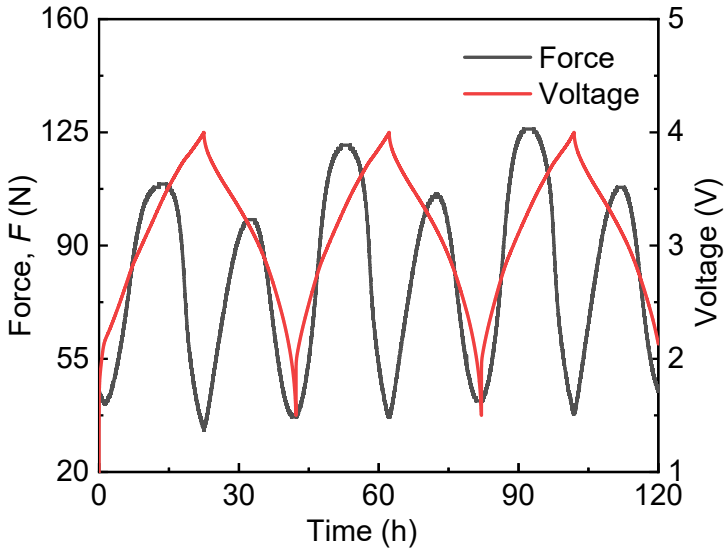

Fig. S2 Evolution of swelling force and cell voltage as a function of time during cycling under a preloading force of 45 N and a current of 10 mA. The force signal exhibits periodic variation that correlates with the charge-discharge process, while the voltage profile shows the corresponding electrochemical cycling behavior over repeated cycles.

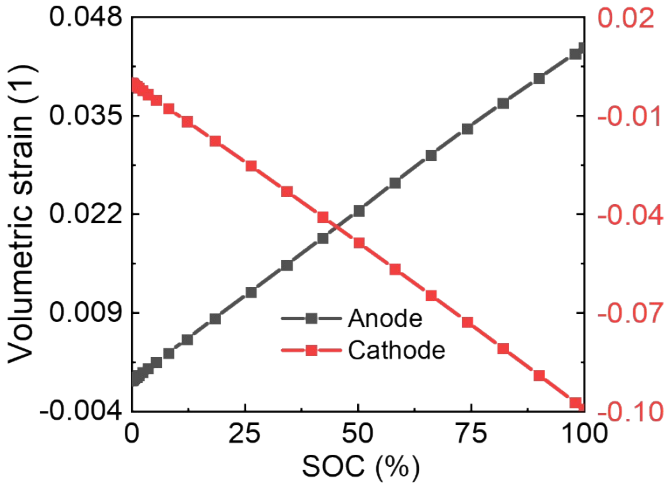

Fig. S3 Evolution of volumetric strain in the anode and cathode particle as a function of state of charge, highlighting monotonic anode expansion and cathode shrinkage during cycling.

References

[1] B. Liu, Y. Jia, J. Li, S. Yin, C. Yuan, Z. Hu, L. Wang, Y. Li, J. Xu, J. Mater. Chem. A 6 (2018) 21475–21484.
[2] H. Li, D. Zhou, M. Zhang, B. Liu, C. Zhang, Energy 263 (2023) 126027.
[3] X. Feng, X. He, M. Ouyang, L. Wang, L. Lu, D. Ren, S. Santhanagopalan, J. Electrochem. Soc. 165 (2018) null.
[4] P.T. Coman, E.C. Darcy, C.T. Veje, R.E. White, J. Electrochem. Soc. 164 (2017) A587.
[5] M. Doyle, J. Newman, A.S. Gozdz, C.N. Schmutz, J.-M. Tarascon, J. Electrochem. Soc. 143 (1996) 1890.
[6] M. Doyle, T.F. Fuller, J. Newman, J. Electrochem. Soc. 140 (1993) 1526–1533.
[7] M. Doyle, J. Newman, Electrochim. Acta. 40 (1995) 2191–2196.
[8] K. Chayambuka, G. Mulder, D.L. Danilov, P.H.L. Notten, Electrochim. Acta 404 (2022) 139764.
[9] D. Kim, E. Lee, M. Slater, W. Lu, S. Rood, C.S. Johnson, Electrochemistry Communications 18 (2012) 66–69.